Z. Physik B - Condensed Matter 39, 305–310 (1980)

Condensed Matter
Zeitschrift für Physik B

Structural and Magnetic Phase Transitions in $TbPO_4$ Studied by Neutron Diffraction

W. Nägele[1], D. Hohlwein[1], and G. Domann[2]
[1] Institut für Kristallographie der Universität, Tübingen, Federal Republic of Germany
[2] Physikalisches Institut der Universität, Karlsruhe, Federal Republic of Germany

Received May 16, 1980

Neutron diffraction experiments on $TbPO_4$ single crystals have been performed in the temperature range from 1.35 to 294 K. We observe two phase transitions: the onset of antiferromagnetic ordering along the tetragonal c-axis at 2.28 K and tilting of the moments away from the c-axis below 2.15 K. The analysis of the measured reflection profiles shows that the tilting is connected with a distortion of the tetragonal zircon structure.

I. Introduction

The rare earth arsenates, vanadates, and phosphates undergo interesting phase transitions at low temperatures. Whereas at room temperature they exhibit the tetragonal zircon structure (Fig. 1), some of them change their symmetry to orthorhombic below 40 K. These structural transitions are induced by a cooperative Jahn-Teller effect [1]. At temperatures below 10 K some compounds undergo magnetic ordering. There are substances which show both kinds of transitions and others with only one either structural or magnetic. These phase transitions and the associate phase diagrams and critical points have been studied in many compounds. In some systems they have been well understood and could be explained in terms of elaborate theories.

One of the less understood systems is $TbPO_4$, although many authors have dealt with this subject during the past decade [2]. Two phase transitions have been observed by different experimental methods. At the early stage of investigation the reported transition temperatures showed considerable deviations, but the influence of external stress (due to the sample mounting) on the transitions was soon recognized. By a careful study of the linear optical birefringence reliable transition temperatures were obtained [3] which could be confirmed by measurements of the specific heat [4, 5]: a first transition at $T_1^c = (2.28 \pm 0.02)$ K followed by a second one at $T_2^c = (2.15 \pm 0.02)$ K. There seems to be no doubt that well below 2.15 K the system is antiferromagnetic with a colinear spin structure tilted off the c-axis within the (110) plane. Different values of the tilt angle between the magnetic moments and the c-axis have been reported by different authors. It is also not clear whether a lattice distortion is followed by magnetic ordering or vice versa or whether both transitions are purely magnetic or magnetic and coupled with a lattice distortion. To elucidate these questions we have performed neutron diffraction experiments on $TbPO_4$ single crystals which will be reported in this paper.

II. Experimental Details

The neutron diffraction experiments were performed at the research reactor FR2, Kernforschungszentrum Karlsruhe, using the P14 powder diffractometer (high resolution) at a neutron wavelength of 1.028 Å in a single crystal configuration. The $TbPO_4$ single crystals (typical dimensions $4 \times 2 \times 1$ mm^3) were grown by a flux method [6] by Dr. Wendl and Dr. Müller-Vogt (Kristall- und Materiallabor, Universität Karlsruhe). The large crystal faces were (100) and (010) planes,

0340-224X/80/0039/0305/$01.20

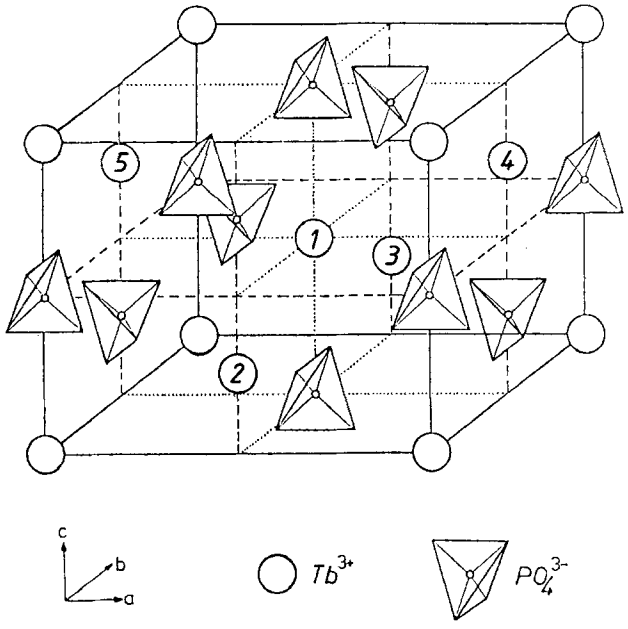

Fig. 1. Tetragonal unit cell of $TbPO_4$ with four formula units. The space group is $I4_1/amd$, and the point symmetry of Tb^{3+} is $\bar{4}m2$. Each Tb^{3+} ion (e.g. 1) has four nearest Tb^{3+} neighbours (labelled 2–5)

whereas the small faces were (101) and (011) some of them irregularly broken. A crystal was glued to an aluminium needle which was mounted on a goniometer head. To minimize external stress a very small quantity of glue was used. The crystal was preoriented with a recently developed neutron Laue-camera [7], and the goniometer head was then attached to a vertical axis inside a ^4He bath cryostat. The crystal was surrounded by liquid ^4He. By pumping on the ^4He reservoir temperatures down to 1.35 K were reached. They were controlled via a calibrated 100 Ω Allen-Bradley carbon resistor and stabilized by a PID controller. The absolute accuracy of temperature was about 0.01 K with a stability of better than 0.005 K during one measurement. The crystal could be rotated around the vertical axis by an external computer-controlled turn-table (step width 0.005°) which was mounted on top of the cryostat. With two orientations of the crystal we measured reflections within the *a-b* and *a-c* plane.

To optimize the peak-to-background ratio a Soller collimator was used in front of the detector. This collimator (20′) cuts off different proportions of the reflections at different scattering angles, and therefore the integrated intensities of the reflections ar not on the same scale. However, as we are only interested in the temperature dependence of selected reflections, we do not need scaled intensities.

III. "Order Parameter" Measurements

With the *a-b* crystal plane parallel to the scattering plane we first studied the intensity of the (110), (310), and (510) reflections as a function of temperature (indexing is based on the tetragonal unit cell with $a_0 = 6.942$ Å and $c_0 = 6.064$ Å at 6 K [2]). These special reflections $hk0$ with $h, k \neq 2n$ are most suitable to magnetic order parameter studies, as they are forbidden in the zircon structure because of the extinction rule due to the *a*-glide plane perpendicular to ⟨001⟩.

With the *a-c* crystal plane parallel to the scattering plane we studied the intensity of the (002) and (101) reflections. Due to the 4_1 screw axis the (002) reflection is also forbidden. The (101) reflection could be studied as its nuclear structure factor is nearly zero due to the scattering lengths of the elements involved.

The integrated intensities were obtained by ω-scans. Figure 2 shows the observed temperature dependence of some of these reflections. We find a different behaviour of the (110), (310), (510), and (101) reflections compared to the (002) reflection as a function of temperature. Looking at (110), (310), (510),

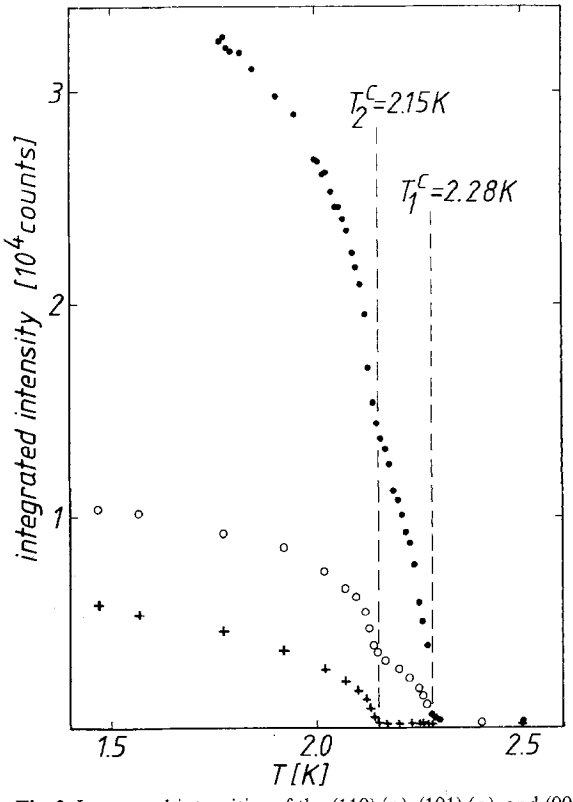

Fig. 2. Integrated intensities of the (110) (●), (101) (○), and (002) (+) reflections

and (101), the onset of scattered intensity is found at about 2.28 K, indicating the first transition. A change of the slope of the intensity vs. temperature curve at 2.15 K indicates the second transition. The (002) reflection, however, can be observed only below 2.15 K.

These transition temperatures are in excellent agreement with the specific heat results of Schwab and Kahle [4].

To explain the observed results the neutron magnetic scattering cross-section has to be considered. For an ordered array of colinear magnetic moments the intensity is proportional to

$$F_{\text{mag}}^2 \cdot \sin^2\beta$$

where F_{mag} is the magnetic structure factor and β is the angle between the scattering vector τ and the magnetic moment **m.** As the magnetic structure factor of (002) is not equal to zero, the absence of (002) between 2.28 and 2.15 K implies that β is zero in this temperature range. This means that the ordering direction is the tetragonal c-axis. The onset of the (002) intensity below 2.15 K indicates that the moments become tilted off the c-axis. The tilt angle can be obtained in principle from the intensities of (002) and (110). If we define α as the angle between the magnetic moment and the tetragonal c-axis we obtain the intensities

$$I_{hkl} = s \cdot L_{hkl} \cdot E_{hkl} \cdot m^2 \cdot \sin^2\beta \cdot \Big| \sum_{\text{moments}} \hat{e}_i \cdot \exp\{2\pi i(hx_i + ky_i + lz_i)\}\Big|^2$$

where s is a scaling factor, L_{hkl} the Lorentz factor, $\hat{e}_i$ a unit vector in the direction of the magnetic moment and $\mathbf{r}_i = (x_i, y_i, z_i)$ the fractional coordinates of the i-th moment within the unit cell. E_{hkl} is the extinction factor which depends in a complicated way on the crystal mosaic structure, the structure factor of hkl and the mean path length of the neutron beam within the crystal.

If we set up the ratio $R = I_{002}/I_{110}$ we obtain

$$R = \frac{s \cdot L_{002} \cdot E_{002} \cdot m^2 \cdot \sin^2\alpha \cdot \big|\sum_i \hat{e}_i \cdot \exp\{4\pi i z_i\}\big|^2}{s \cdot L_{110} \cdot E_{110} \cdot m^2 \cdot \cos^2\alpha \cdot \big|\sum_i \hat{e}_i \cdot \exp\{2\pi i(x_i + y_i)\}\big|^2} = C \cdot \tan^2\alpha$$

(If the crystal structure changes to monoclinic as concluded later, the (110) reflection consists of two symmetrically non-equivalent reflections (110) and $(1\bar{1}0)$ which belong to different domains. This was neglected.)

This ratio was calculated from the observed intensities of (002) and (110). It is plotted in Fig. 3 as a function of temperature, and we can see that the angle α is continuously becoming larger below 2.15 K indicating a second order transition. This temperature dependence may be the explanation why the tilt-off angles given in the literature are different. As E_{hkl} can not easily be determined the absolute values of α should be calculated from powder diffraction data as E_{hkl} is in general unity in this case.

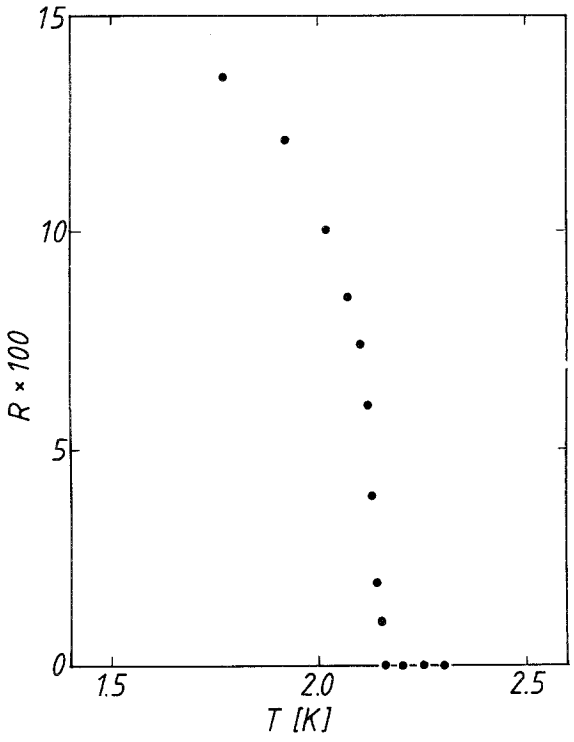

Fig. 3. $R = C \cdot \tan^2\alpha$ as a function of temperature (see text)

A non-zero angle α is not compatible with the point symmetry $\bar{4}m2$ of the Tb^{3+} ions. Therefore at 2.15 K the crystal structure must change to allow the tilted moments.

IV. Analysis of the Reflection Profiles

The change of the crystal structure can be studied by an analysis of the reflection profiles which are obtained by moving the reciprocal lattice points through the Ewald sphere, e.g. by a rotation of the crystal around a vertical axis with fixed detector position (ω-scan). A small distortion of the tetragonal lattice to some orthorhombic or lower symmetry will produce domains of different orientations. So the corresponding reciprocal lattice points of different domains will cross the Ewald sphere at different crystal orientations leading to a splitting $\Delta\omega$ of the reflection profile (Fig. 4). A purely magnetic ordering

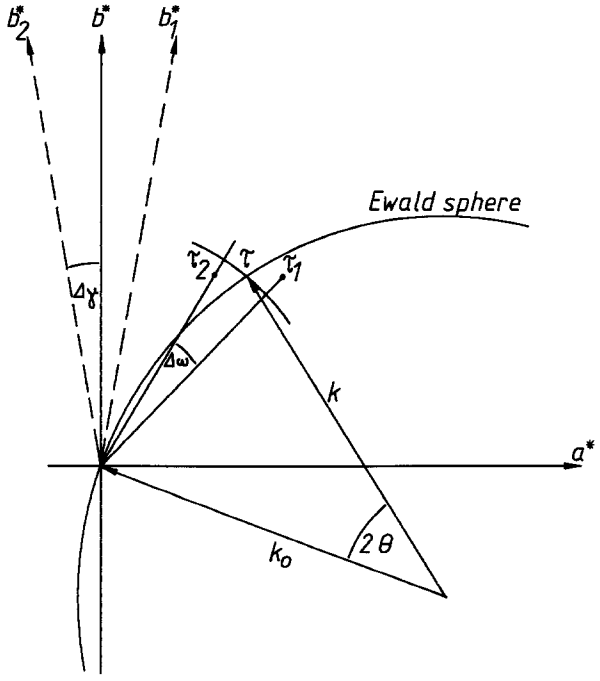

Fig. 4. Schematic representation of an ω-scan through the reciprocal lattice point τ which is split into τ_1 and τ_2 by the lattice distortion $\Delta\gamma$. This distortion angle leads to a splitting $\Delta\omega$ of the reflection profile

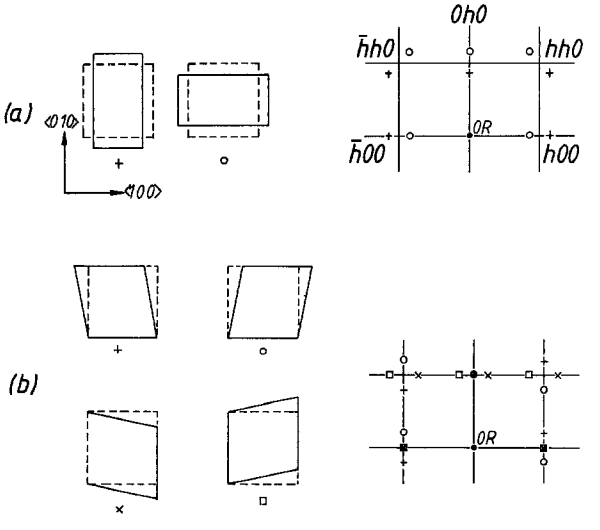

Fig. 5. Illustration of orthorhombic and monoclinic distortions of the tetragonal basal plane (left hand side) and their effect on the reciprocal lattice (right hand side). (a) orthorhombic distortion along the tetragonal axes, (b) monoclinic distortion along the tetragonal axes. (OR = origin of the reciprocal lattice)

within the tetragonal unit cell will not change the reflection profiles.

In Fig. 5 we have shown the possible orthorhombic and monoclinic distortions of the basal plane of the tetragonal lattice. The resulting domains lead to the construction of the corresponding reciprocal lattices which are drawn with different symbols in the same diagram. The effect of these distortions on the reflection profiles of an ω-scan will be discussed in the following. An ω-scan is best suited for the neutron-diffractometer because the resolution is in general better in ω than in the scattering angle 2θ.

a) Orthorhombic Distortions

The distortion along ⟨100⟩ (Fig. 5a) leads to a splitting of all $hk0$ reflections with the exception of $h00$ and $0k0$ in an ω-scan. (We assume a small distortion only so that the scattering angles 2θ can be considered to remain unaffected by this distortion.) The ⟨110⟩ distortion can be visualized by a 45° rotation of Fig. 5a. In this case the $hh0$ reflections do not split, and the split $h00$ and $0h0$ profiles should be mirror images or identical. If we combine the ⟨110⟩ distortion with small rotations of the domains, so that always a principal axis of the original lattice is conserved, we get four domains. In this case, the distribution of the reciprocal lattice points is very similar to the case of monoclinic distortions discussed next.

b) Monoclinic Distortions

A monoclinic distortion of the basal plane which leaves the a-axis invariant yields maximum splitting for $h00$ reflections, whereas $0h0$ reflections do not split (+ and ○ in Fig. 5b). If the b-axis is left invariant (× and □) $0h0$ reflections split and $h00$ is unaffected. In both cases the splitting of $hh0$ and $\bar{h}h0$ reflections is smaller than that of $h00$ and $0h0$, respectively. A combination of both distortions leads to a triplet structure of $h00$ and $0h0$ reflections. If the domain distribution is not uniform the triplet structure of corresponding $h00$ and $0h0$ reflections need not to be identical. The monoclinic distortions which leave one diagonal of the basal plane invariant give the same result if we replace $h00$ by $hh0$ and $0h0$ by $\bar{h}h0$.

Figure 6 shows ω-scans of the (600), (060), and (440) reflections for different temperatures. They were measured with the a-b crystal plane parallel to the scattering plane. These reflections are not affected by the magnetic ordering as their magnetic structure factors are zero [2]. So they are only sensitive to structural changes. At high temperatures we observed an approximately Gaussian line shape which is the convolution of the Gaussian resolution function of the diffractometer and the crystal mosaic distribution. The reflection intensities and profiles are not in-

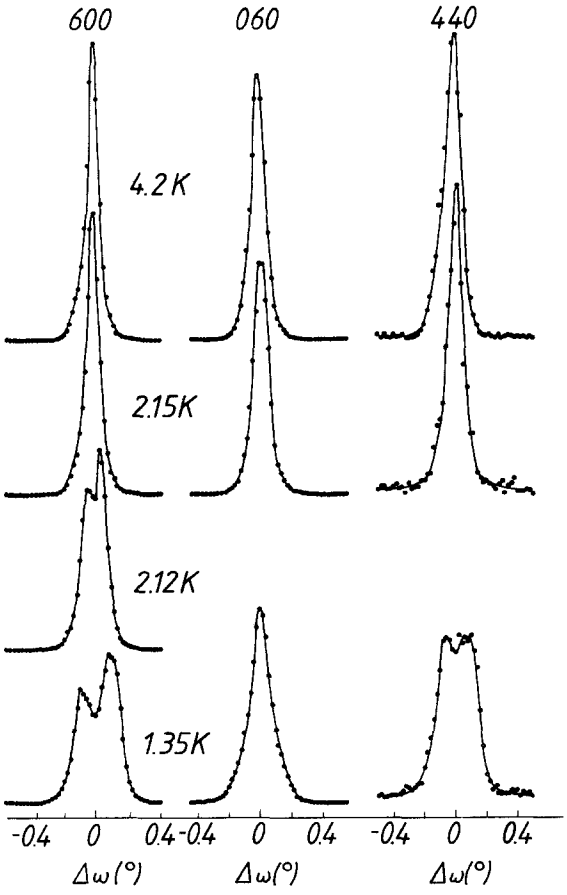

Fig. 6. Reflection profiles of (600), (060), and (440) at different temperatures

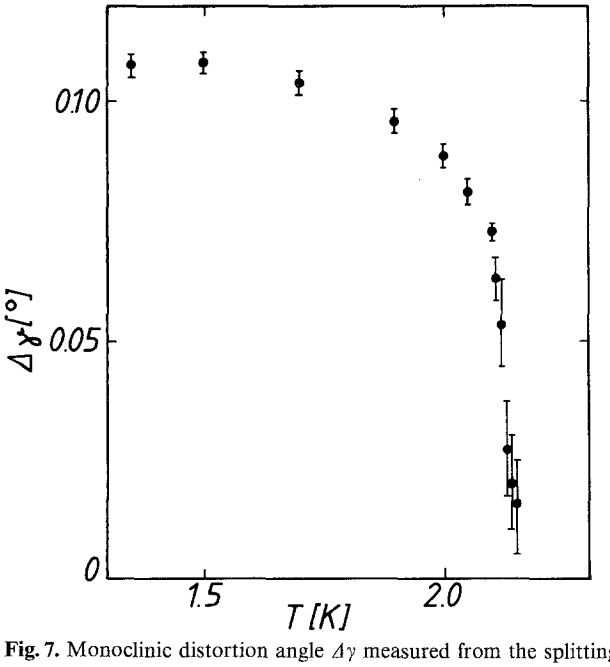

Fig. 7. Monoclinic distortion angle $\Delta\gamma$ measured from the splitting of the (600) reflection

fluenced by the first transition at 2.28 K, but the profiles appreciably change below 2.15 K: they are increasingly split. Therefore the transition at 2.28 K is a purely magnetic one with antiferromagnetic ordering along the tetragonal c-axis. The tilting of the moments off the c-axis below 2.15 K, however, is connected with a lattice distortion at 2.15 K.

As the measured splitting of (600) and (060) is larger than that of (440) we can exclude the orthorhombic distortions along $\langle 100\rangle$ and $\langle 010\rangle$. As at low temperatures three Gaussians contribute significantly to the profiles of (600) and (060), the splitting should be due either to the orthorhombic $\langle 110\rangle$-distortion with four domains or the monoclinic distortions which shear the unit cell along the tetragonal axes. The monoclinic magnetic structure below 2.15 K [2], however, suggests that the distortion is monoclinic.

A further splitting of reflections within the a-c crystal plane which would have indicated a triclinic distortion could not be observed.

The monoclinic distortion angle $\Delta\gamma$ is half the splitting $\Delta\omega$ of reflections on the reciprocal axes as can be seen from Fig. 5. $\Delta\omega$ was determined from the (600) splitting by a fit of three Gaussians with the fixed instrumental linewidth determined at 294 K to the profile. The resulting $\Delta\gamma$ is given in Fig. 7. The large error bars above 2.11 K are due to the fact that the three lines are no longer resolved but form a broad line together. This introduces strong correlations between the fit parameters thus leading to large standard deviations. Therefore we consider it impossible to derive from the splitting vs. temperature curve whether the lattice distortion is continuous or not. To test the consistency we compared the measured splitting of several non-axial reflections ((440, (310) etc.) with that computed from the monoclinic domains with axes $a=b=a_0$, $c=c_0$ and monoclinic angles $90°\pm\Delta\gamma$. The agreement was within the experimental error.

V. Conclusion

Our neutron diffraction experiments have confirmed the two phase transitions observed by Becker and Keller [3], Schwab and Kahle [4], and Suzuki and Nakajima [5]. We have shown that the transition at 2.28 K is purely magnetic with antiferromagnetic ordering along the tetragonal c-axis. The transition at 2.15 K is due to tilting of the magnetic moments off the c-axis together with a monoclinic lattice distortion within the a-b plane. Both tilt-off angle α and monoclinic distortion angle $\Delta\gamma$ increase with decreasing temperature. But it becomes not fully clear whether the transition at 2.15 K is of first or second order.

Fruitful discussions with professors Kahle and Prandl and Dr. Kasten improved the original manuscript. We are indebted to the Kernforschungszentrum Karlsruhe for allocation of neutron beam time and technical assistance. This work was supported by the Bundesministerium für Forschung und Technologie (project KNF 03-41 E 03 P; 04-45 E 03 I).

References

1. For a review see: Gehring, G.A., Gehring, K.A.: Rep. Prog. Phys. **38**, 1 (1975)
2. Coing-Boyat, J., Sayetat, F., Apostolov, A.: J. Phys. (Paris) **36**, 1165 (1975) (and references therein)
3. Becker, P.J., Keller, E.: (to be published)
4. Schwab, M., Kahle, H.G.: Phys. Status Solidi B**84**, 167 (1977)
5. Suzuki, H., Nakajima, T.: J. Phys. Soc. Jpn. **47**, 1441 (1979)
6. Hintzmann, W., Müller-Vogt, G.: J. Cryst. Growth **5**, 274 (1969)
7. Hohlwein, D.: KfK-Report 2719, p. 75 (1978). Kernforschungszentrum Karlsruhe (unpublished)

W. Nägele
D. Hohlwein
Institut für Kristallographie der Universität Tübingen
Charlottenstr. 33
D-7400 Tübingen
Federal Republic of Germany

G. Domann
Physikalisches Institut der Universität Karlsruhe
Engesserstr. 7
D-7500 Karlsruhe
Federal Republic of Germany